Local Flexoelectricity and Magnetism in Strain-Gradient Rare-Earth Iron Garnet Thin Films

Garnet-structured ferrimagnetic insulator $Sm_3Fe_5O_{12}$ thin films were grown on $Gd_3Ga_5O_{12}$ substrates by pulsed laser deposition. The $Sm_3Fe_5O_{12}$ films showed coherently strained-tetragonal, strain-gradient at around dislocations, and relaxed-cubic structures from the interface to the surface depending on the film thickness due to the epitaxial strain and lattice relaxation. The local electronic structure and magnetic properties were investigated by XMCD, which revealed the presence of flexoelectric polarization and magnetization under the inhomogeneous strain distribution. We believe this study paves the way for achieving dielectric polarization even in centrosymmetric materials by strain engineering.

Ferrimagnetic insulators of rare-earth iron garnets (RIGs, $R_3Fe_5O_{12}$) have rich magnetic characteristics of the large magneto-optical effect and spin-wave propagation with exceptionally low damping constant. The control of magnetic anisotropy has been one of the key challenges for spintronics applications. In garnet thin films, not only magnetocrystalline anisotropy but also magnetic shape anisotropy and magnetoelastic anisotropy contribute to the effective anisotropy [1]. The shape anisotropy for the films prefers an in-plane magnetic easy axis, while the magnetoelastic anisotropy described as $K_u = -3/2(\lambda\sigma)$ can exhibit perpendicular magnetic anisotropy (PMA) depending on the magnetostriction constants λ and in-plane stress σ. In addition to the magnetoelastic anisotropy, strain engineering is a possible approach to induce and/or enhance ferroelectricity. However, the RIG films belong to the centrosymmetric $I4_1/acd$ (tetragonal) or $Ia3d$ (cubic) space group under homogeneous epitaxial strain, which cannot represent remnant dielectric polarization [2]. Thus, we hypothesized that inhomogeneous strain could break local centrosymmetry and show flexoelectric polarization expressed as $P_{\text{Flexoelectricity}} = \mu\partial u/\partial x$, where μ and $\partial u/\partial x$ represent the flexoelectric coefficient and strain-gradient [3]. If remnant magnetization and dielectric polarization coexist in RIGs, simultaneous ordering of dipoles and spins is expected in addition to the magneto-electric correlation, which would be a promising material for future spintronics applications.

In this study, $Sm_3Fe_5O_{12}$ (SmIG) films with various thicknesses were grown on $Gd_3Ga_5O_{12}$ (GGG) (001) substrates by pulsed laser deposition [4]. The lattice mismatch and critical thickness t_c where misfit dislocation occurs are estimated as –1.2% and 60 nm, respectively. The SmIG films grown on GGG (001) substrates are expected to show PMA because of the compressive strain and positive λ. Reciprocal space mapping (RSM) for films with thickness $t < t_c$ exhibits coherent epitaxy and tetragonal elongation [Fig. 1(a)]. As t increases to 60 nm, the strain starts to relax, and the diffraction peak shifts from tetragonal to relaxed-cubic. For further structural characterization, we performed scanning transmission electron microscopy (STEM) for the sufficiently-thick film (t = 180 nm). The micrometer-scale imaging shows lateral crystalline uniformity in the thickness range of 50 nm or less and abrupt contrast change originating from dislocations above this [Fig. 1(b)]. Figures 1(c) and (d) show high-magnification images around the interface and dislocations, respectively. Fully coherent growth is observed at the SmIG/GGG interface. At around the dislocations, vertical lattice constants are homogeneous over the image, while lateral ones gradually increase with film thickness. The tetragonal lattice distortion defined as c/a indicates gradual strain relaxation further away from the substrate. A simple linear extrapolation predicts the relaxation thickness of 15 nm, corresponding to strain-gradient $\partial u/\partial x = 9\times10^5$ m^{-1} [Fig. 1(e)]. Negatively polarized local domains with average diameter of 30 nm are observed in the strain-gradient by scanning nonlinear dielectric microscopy (SNDM) [Fig. 1(f)] on the surface.

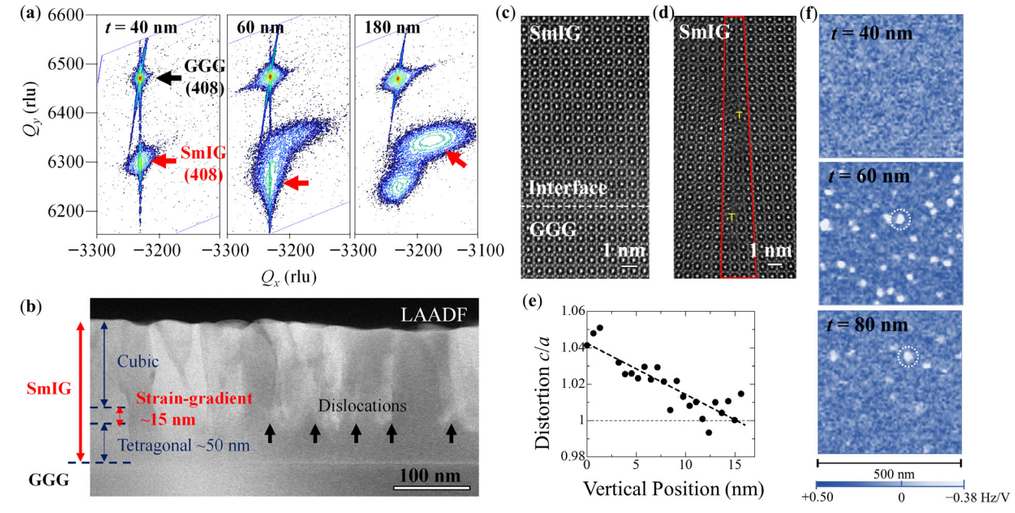

Figure 1: (a) RSM around (408) substrate peaks for 40, 60, and 180 nm-thick SmIG films. Q_x and Q_y indicate reciprocal lattice unit (rlu) along (100) and (001), respectively. (b–e) STEM analysis of 180 nm-thick SmIG film. (b) Micrometer-scale low-angle annular dark-field (LAADF)-STEM image. Dislocations are denoted by black arrows. (c–d) Nanometer-scale high-angle annular dark-field (HAADF)-STEM images around the SmIG/GGG interface and dislocations. (e) Variation in tetragonal distortion c/a for vertical positions quantified from Fig. 1(d). (f) SNDM images for 40, 60, 80 nm-thick SmIG films. Representative dielectric domains are circled by broken white lines in 60 and 80 nm-thick films.

Magnetic circular dichroism (MCD) for t < 40 nm shows rectangular hysteresis with coercive field H_c < 0.05 T indicating PMA [Fig. 2(a)]. The thickness dependence of H_c is summarized in Fig. 2(b). We elucidated the depth profile of the magnetic properties by X-ray magnetic circular dichroism (XMCD). Surface-sensitive total-electron-yield (TEY) measurements for t = 40, 45, 110 nm films reveal the local electronic and magnetic structures in the tetragonal, strain-gradient, and cubic phases in contrast with bulk-sensitive MCD measurements. Figure 2(c) shows the Fe $L_{2,3}$-XMCD spectra. The spin (M_{spin}), orbital (M_{orb}), and total (M_{tot}) magnetic moments are estimated by XMCD sum rules. The non-zero values of M_{orb} for the 40 and 45 nm-thick films indicate that the quenching of orbital moments is resolved by the reduction of the crystal symmetry from cubic to tetragonal and strain-gradient. The magnetic-field dependence of the XMCD intensity in TEY mode exhibits clear hysteresis. The XMCD hysteresis of the partially relaxed 45 nm-thick film is at H_c = 0.11 T, while that of the 20 and 110 nm-thick films is at H_c = 0.02 T. Ferrimagnetism and increased magnetic coercivity due to magnetic domain pinning by dislocations were observed in the strain-gradient layer. These results demonstrate that strain-gradient SmIG possesses both remnant dielectric polarization and magnetization at room temperature. Our study not only suggests the possible application of multifunctional materials with remnant magnetization and dielectric polarization, but also paves the way for producing polar nanodomains even in centrosymmetric crystals by controlling singularity structures including dislocations.

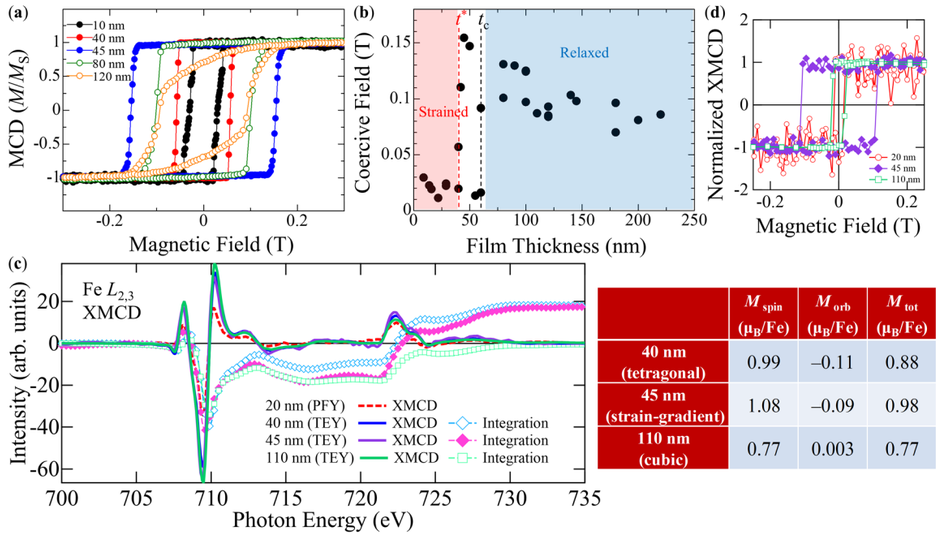

	M_{spin} (μ_B/Fe)	M_{orb} (μ_B/Fe)	M_{tot} (μ_B/Fe)
40 nm (tetragonal)	0.99	–0.11	0.88
45 nm (strain-gradient)	1.08	–0.09	0.98
110 nm (cubic)	0.77	0.003	0.77

Figure 2: (a) Magnetic hysteresis loops of MCD with the field applied perpendicular to the film surface for 10, 40, 45, 80, 120 nm-thick SmIG films. (b) Thickness dependence of H_c measured by MCD. t_c (60 nm) and $\dot{t}$ (40 nm) represent the critical thickness estimated from the bulk lattice constant and the thickness where relaxation starts as estimated from structural analysis. (c) Fe $L_{2,3}$-XMCD spectra. The XMCD spectra were obtained in the total-electron-yield (TEY) mode except for the 20 nm-thick film, which was obtained in the partial-fluorescence-yield (PFY) mode. The table summarizes spin (M_{spin}), orbital (M_{orb}), and total (M_{tot}) magnetic moments estimated by XMCD sum rules. (d) Magnetic hysteresis loops of XMCD intensity for 20, 45, 110 nm-thick films at room temperature.

REFERENCES

[1] C. Holzmann, A. Ullrich, O. -T. Ciubotariu and M. Albrecht, *ACS Appl. Nano Mater.* **5**, 1023 (2022).
[2] P. Baettig and T. Oguchi, *Chem. Mater.* **20**, 7545 (2008).
[3] P. Zubko, G. Catalan and A. K. Tagantsev, *Annu. Rev. Mater. Res.* **43**, 387 (2013).
[4] H. Yamahara, B. Feng, M. Seki, M. Adachi, Md S. Sarker, T. Takeda, M. Kobayashi, R. Ishikawa, Y. Ikuhara, Y. Cho and H. Tabata, *Commun. Mater.* **2**, 95 (2021).

BEAMLINE

BL-16A

H. Yamahara[1], B. Feng[1], M. Seki[1], M. Adachi[1], Md S. Sarker[1], T. Takeda[1], M. Kobayashi[1], R. Ishikawa[1], Y. Ikuhara[1], Y. Cho[2] and H. Tabata[1] ([1]The Univ. of Tokyo, [2]Tohoku Univ.)